Chapter 1
From Metal Particles to Property-Mapped Linear Feedstock via Cyclic Shear Solid-State Consolidation



DISTRIBUTION STATEMENT A: Approved for Public Release, Distribution Unlimited.

Mohamed A. Abbas, M Faisal Riyad, Christopher Suter, Nathan Fonseca, Shams Torabnia, Pu Han, and Keng Hsu

Abstract Wire-fed and extrusion-based additive manufacturing (AM) processes rely on linear feedstock materials, including wires, rods, billets, and strips. Establishing mechanical property gradients in these feedstocks permits control of on-site mechanical properties in AM components and reduces defects associated with stress concentrations. Conversion of metal particles into linear feedstocks is primarily achieved by melting processes or by solid-state consolidation. However, the development of property gradients in feedstock produced by existing technologies is inhibited by particle homogenization during conversion. To address this limitation, the present study introduces a novel method for cyclic shear solid-state consolidation for heterogeneous metal particles. This method overlays cyclic shear strain-induced softening, controlled plastic deformation, and solid-state mass transport to convert metal particles into dense, continuous, or discrete linear feedstock without remelting. The process supports precise dimensional control and progressive build-up in both in-plane and out-of-plane orientations. Moreover, the proposed technique facilitates the recycling of reclaimed metal particles from out-of-spec AM powders to machining chips.

Keywords Solid-state consolidation · Cyclic shear · Linear feedstock · Metal conversion · Additive manufacturing

Introduction

Wire-fed and extrusion-based additive manufacturing (AM) use linear feedstocks—such as wires, rods, billets, and strips—to support high deposition rates and scalable AM systems. The internal structure of feedstock directly affects interfacial bonding during deposition and the mechanical performance of AM components. Despite the growing adoption of AM driven by advantages including the fabrication of complex geometries and shorter lead times, substantial limitations continue to impede its widespread industrial implementation. Current AM techniques predominantly rely on pristine feedstock materials, while reclaimed resources such as out-of-specification powders and machining chips remain unexplored. Moreover, many engineering components require site-specific mechanical properties to withstand non-uniform thermal and mechanical loads. While spatial property control is achievable through process-level approaches, including in-situ parameter modulation and toolpath-based control, these methods introduce significant process complexity [1–6].

To address these limitations, this work introduces a novel cyclic shear solid-state consolidation approach that combines repetitive shear strain–induced softening, controlled plastic deformation, and solid-state mass transport to convert heterogeneous metal particles into dense linear feedstock while preserving spatial heterogeneity. This technique enables precise control over feedstock composition, allowing either continuous gradients or sharp transitions between distinct material compositions, as schematically illustrated in Fig. 1. Such feedstock-level control facilitates tailoring of site-specific mechanical properties in AM components along both the longitudinal and transverse directions. Using the proposed approach, strip-form

Mohamed A. Abbas · M Faisal Riyad · Christopher Suter · Nathan Fonseca · Shams Torabnia · Pu Han · Keng Hsu
School of Manufacturing Systems and Networks, Arizona State University, Mesa, AZ 85212, USA
e-mail: mohamed.abbas@asu.edu; faisal.riyad@asu.edu; csuter12@asu.edu; nfonsec1@asu.edu; storabnia@asu.edu; Pu.Han@asu.edu; Keng.H.Hsu@asu.edu

© The Author(s), under exclusive license to River Publishers 2026

Piyush Thakre et al. (eds.), *Mechanics of Additive and Advanced Manufacturing, Inverse Methods and Machine Learning, Volume 5, 2026*, Conference Proceedings of the Society for Experimental Mechanics Series, https://doi.org/10.13052/rp-9788743815983

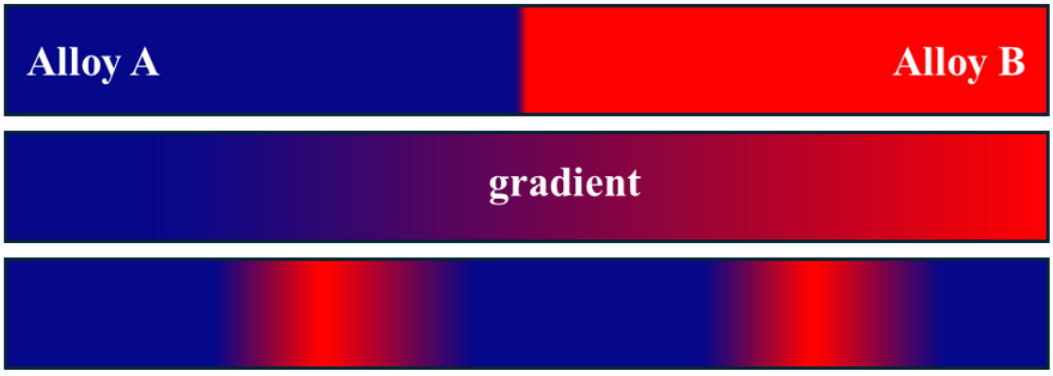

Fig. 1 Potential material composition transition [1, 2].

feedstock was fabricated from a 20 wt.% AA-1100 and 80 wt.% AA-6061 machining chip mixture, thereby establishing the feasibility of feedstock-level compositional control. This approach also has the potential to be scaled and applied to the manufacturing of functionally graded materials (FGMs).

Material preparation

The input material for cyclic shear solid-state consolidation consisted of machining chips from AA-1100 and AA-6061 alloys (O-state), with their chemical compositions summarized in Table 1. The process flow for machining chip production is depicted in Fig. 2. The as-received materials were aluminum plates with average dimensions of 6 in $\times$ 6 in $\times$ 0.125 in. The plates were shredded using CNC milling to produce machining chips as a representative form of reclaimed metal feedstock. The resulting chips were collected and subsequently blended by weight to produce a heterogeneous particle mixture containing 20 wt.% AA-1100-O and 80 wt.% AA-6061-O. This approach allows precise control over composition. The collected chips were not sieved to replicate industrial reclamation conditions. The use of annealed starting materials ensured that the mechanical response of the consolidated feedstock reflected consolidation-induced deformation and microstructural evolution rather than prior thermomechanical strengthening.

Table 1 The chemical composition of AA1100-O and AA6061-O (wt.%).

	Al	Si	Mg	Fe	Cu	Mn	Cr	Ti
AA-1100-O	99.24	0.16	ND	0.3	0.11	ND	ND	ND
AA-6061-O	97.15	0.59	1.23	0.33	0.28	0.07	0.19	0.03

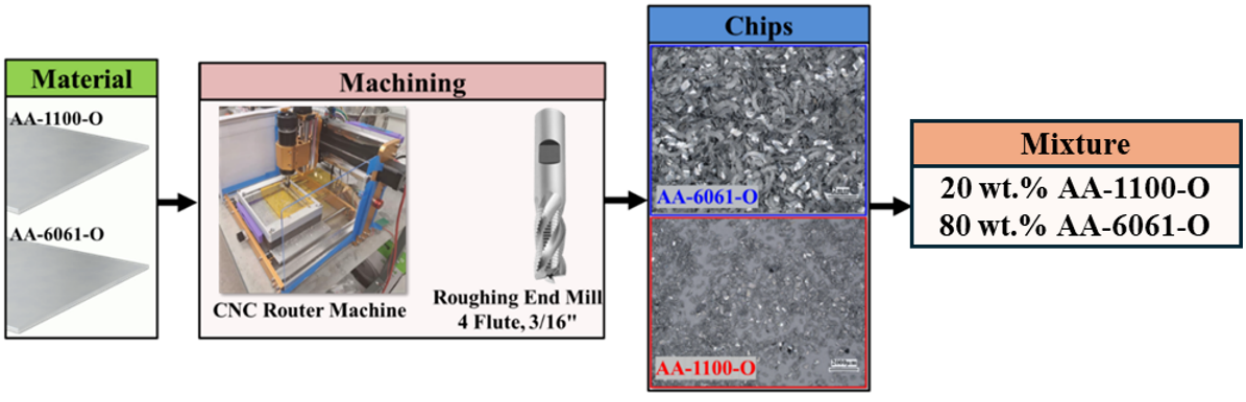

Fig. 2 Process flow for machining chip production.

Cyclic shear solid-state consolidation

The cyclic shear solid-state consolidation setup (Fig. 3) was built on a Tormach PCNC440 CNC milling machine. A D2 tool steel die assembly was mounted to the machine table using M8 bolts, with a mold insert secured by M4 bolts and featuring a 210 mm × 3 mm × 5 mm slot (Fig. 3(b)). Two heating rods embedded in the die core heated the assembly to 400 °C, with temperature regulated by an internal thermocouple. The die was insulated using ceramic fiber and heat-resistant tape. The powder hopper was integrated with a stepper motor–driven gate to provide controlled dispensing of the chips. An ultrasonic transducer operating at 35 kHz and 40% amplitude was mounted to the tool changer base plate and coupled to a horn to deliver acoustic energy into the aluminum particles. The ultrasonic excitation induces cyclic horn oscillations in the Z-direction with an amplitude of 3.675 μm at the mid-section. The horn was fabricated from D2 tool steel and coated with an amorphous diamond layer. Compressed air was supplied to the rear end of the transducer to provide cooling during consolidation, preventing overheating and ensuring stable ultrasonic oscillations.

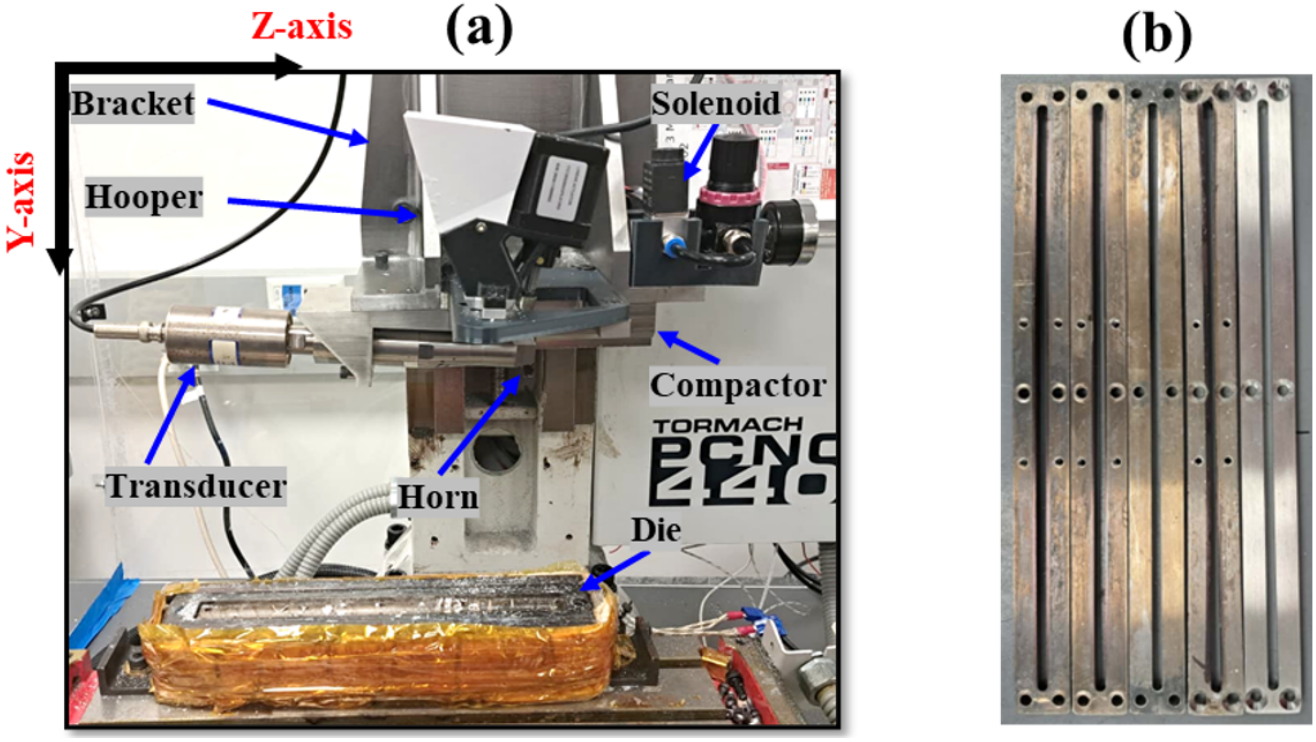

Fig. 3 The setup for cyclic shear solid-state consolidation (a) complete setup, and (b) mold inserts.

To initiate the consolidation process, the mold insert was attached to the die, and heating was applied until a temperature of 400 °C was reached. Once the consolidation temperature was achieved, the hopper was actuated to dispense machining chips into the slot. The chips were then pre-compacted using the compactor to reduce inter-particle spacing and increase the initial packing density. Ultrasonic energy was subsequently applied following the horn motion sequence illustrated in Fig. 4, where the horn first moved vertically to compact the material, held for 0.6 s, and then retracted and translated horizontally by 3 mm to the next segment. This sequence was repeated until all chips within the slot were fully consolidated. Additional layers were built using the same procedure, resulting in a fully bonded multilayer strip. All operations were controlled using a custom-designed G-code implemented on the CNC system.

Results and discussion

In this study, aluminum strips were fabricated by stacking two consolidated layers. The resulting strips had mean dimensions of 210 mm × 4 mm × 2.5 mm, as illustrated in Fig. 5(a) and (b). The observed increase in strip width relative to the slot width is attributed to lateral expansion induced by compressive loading during pre-compaction and consolidation. Representative optical micrographs of the longitudinal and transverse cross sections are shown in Fig. 5(c) and (d). The images confirm

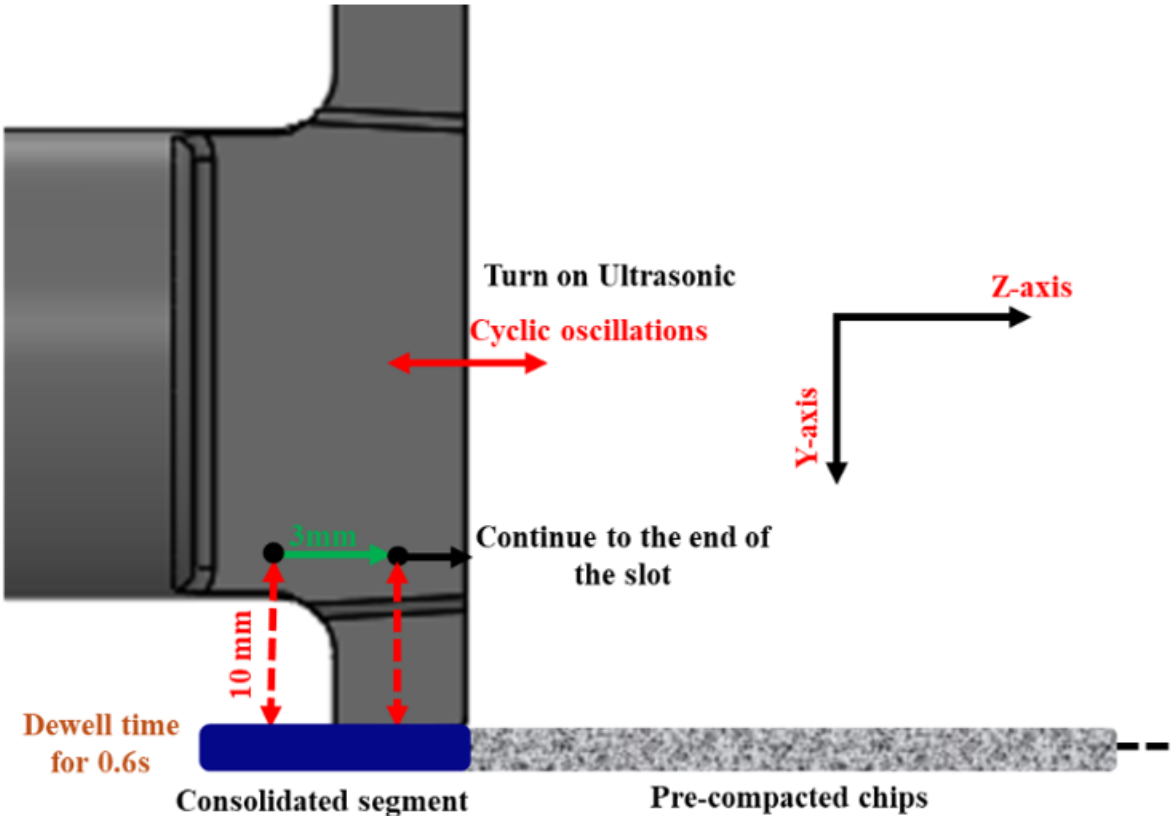

Fig. 4 The sequence for the horn movement during the consolidation process.

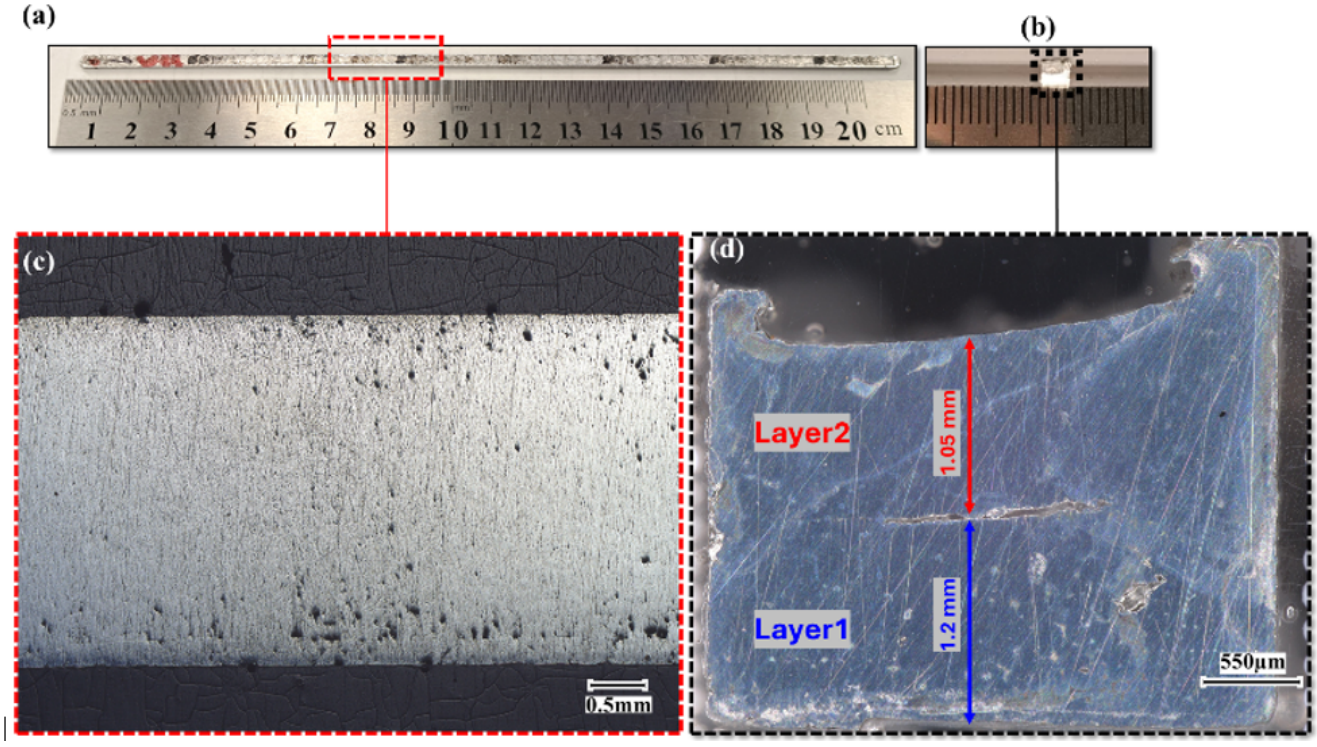

Fig. 5 Consolidated aluminum strip: (a,b) photographs; (c,d) longitudinal and transverse cross-section micrographs.

disruption of the oxide layers surrounding the chips and successful consolidation into a solid feedstock material. However, defects such as voids remain at the lateral boundaries, and incomplete bonding between the two layers is observed. These defects are attributed to the lateral expansion of the mold insert during consolidation, which causes chips in the mid-section to be displaced toward the sides that are not directly compacted by the horn. This displacement reduces the effective compaction pressure in the central region, leading to incomplete interlayer welding.

The microstructure of the aluminium strip was further characterized using EBSD analysis across its cross-section. The EBSD data were post-processed by Aztec Crystal software. Figure 6 (a–c) shows the color-coded grain orientation and distribution map across the cross-section of the strip. As shown in Figure 6 (a), X is the direction of the static shear, Y is the direction of compaction force, and Z, orthogonal to the X-Y plane, is the direction of the applied cyclic shear strain during the consolidation process. The EBSD orientation mapping reveals a nearly continuous and well-bonded microstructure exhibiting an equiaxed grain structure without appreciable elongation along the static shear direction. Figure 6 (d) shows the area-weighted mean grain size to be approximately 2.0 μm, with grain sizes ranging from 1.07 to 5.51 μm. Only sparse, narrow, unindexed features are observed and can be interpreted as residual chip-chip interfaces or isolated pores. Grain continuity across chip boundaries demonstrates effective metallurgical bonding, consistent with oxide disruption and interfacial mass transfer promoted by ultrasonic shear during consolidation. Crystallographic texture analysis using {100}, {110}, and {111} pole figures and inverse pole figures (IPF) along the principal processing directions (X: lateral compaction, Y: compaction, Z: ultrasonic shear) reveals weak overall texture as shown in Figure 6(b and c). Maximum texture intensities do not exceed ∼3.2 multiples of random distribution (m.r.d.), and the texture M-index is 0.067. The pole figures are dominated by broad, diffuse intensity distributions rather than sharp components. The X1 and Y1 IPF display gently varying intensities

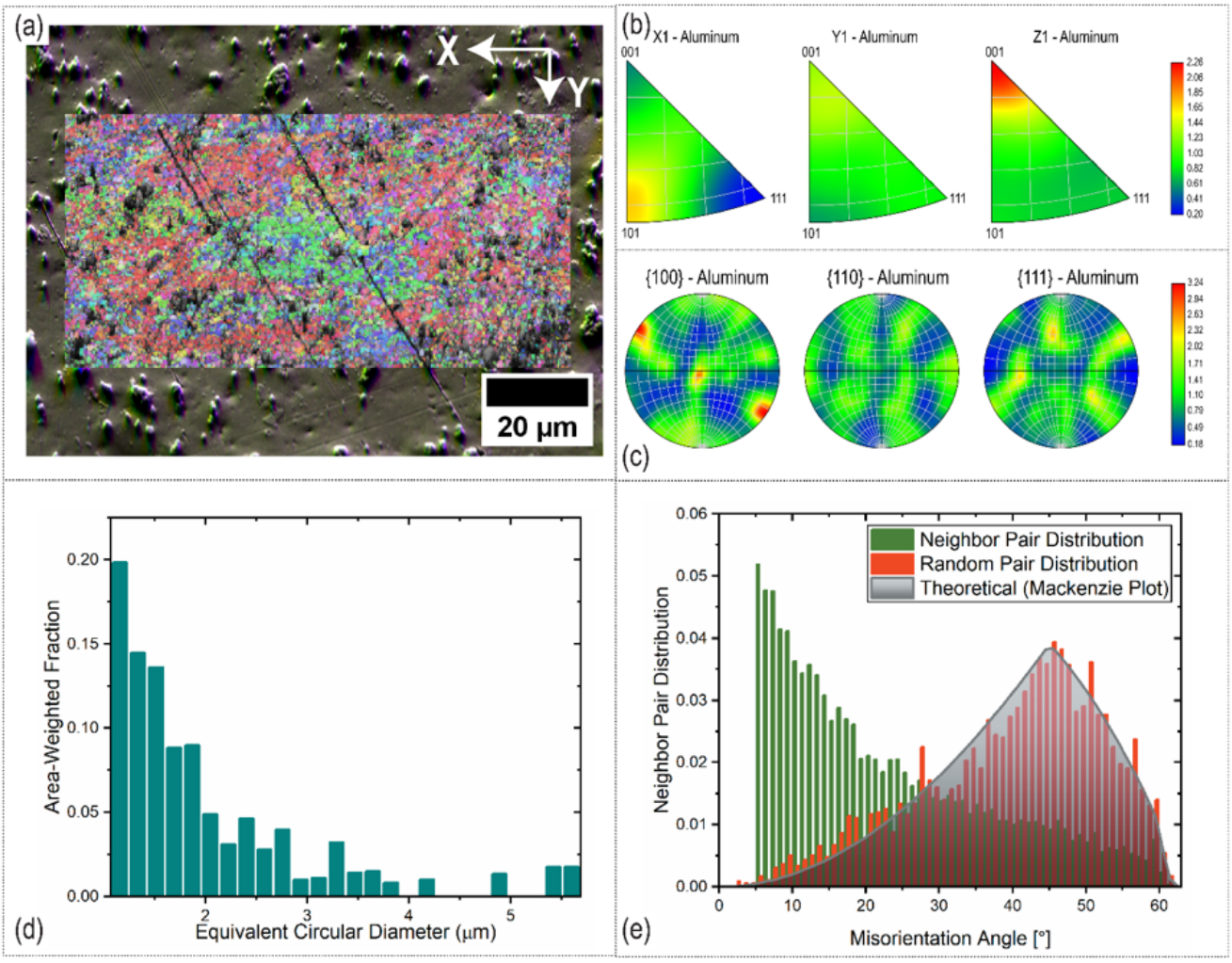

Fig. 6 EBSD analysis of cyclic shear solid-state consolidated AA-1100/AA-6061 machining-chip mixture (a) color-coded grain map (b) inverse pole figure (c) pole figure (d) grain size distribution and (e) misorientation angle analysis.

between $\langle 001 \rangle$, $\langle 101 \rangle$ and $\langle 111 \rangle$, with no strong clustering along any specific direction, suggesting that both compaction directions are nearly randomly oriented with respect to the crystal lattice. By contrast, the Z1 IPF exhibits a modest maximum at the $\langle 001 \rangle$ corner ($\approx$2.3 m.r.d.), indicative of a weak $\langle 001 \rangle$ fibre component parallel to the direction of ultrasonic shear.

Misorientation analysis shown in Figure 6 (e) provides insight into the underlying deformation mechanisms. The neighbor-pair misorientation distribution is strongly biased toward low angles compared with the theoretical MacKenzie distribution and the random-pair distribution. Approximately 40% of neighboring boundaries exhibit misorientations below 15°, and the mean neighbor-pair misorientation angle is $\sim$22.8°, significantly lower than that expected for a random FCC polycrystal [7]. In contrast, the random-pair distribution shows 99% congruence with theoretical predictions, confirming that the excess of low-angle boundaries arises from true microstructural correlations rather than sampling bias. The characteristic orientation domain size, $\sim$4.0 μm, exceeds the mean grain size, indicating that many grains contain internal subgrain structures formed by recovery processes. The absence of a pronounced peak near 60° suggests that annealing twins are not a dominant feature.

In combination, the EBSD results show that the cyclic shear solid-state consolidation converts the heterogeneous chips into a consolidated bulk material with fine equiaxed grain structure, a high density of low-angle subgrain boundaries and weak crystallographic texture. The nearly random orientation distribution and the absence of strong shape or crystallographic texture along the compaction axes suggest that the severe, high-frequency shear associated with ultrasonic excitation effectively erases the deformation and texture inherited from the original chips. The resulting microstructure, ultrafine grains separated by a mixed LAB/HAGB network and aligned along the cyclic shear direction, is expected to provide a relatively isotropic mechanical response combined with grain boundary strengthening and is therefore favorable for structural applications.

Conclusion and Future Work

This study introduced a cyclic shear solid-state consolidation approach for converting heterogeneous metal particles into dense, linear feedstock while preserving spatial heterogeneity. A mixture of 20 wt.% AA-1100 and 80 wt.% AA-6061 machining chips was successfully consolidated, demonstrating the feasibility of feedstock-level compositional control. Microstructural analysis confirmed oxide layer disruption, inter-chip bonding, and a fine equiaxed grain structure. Although incomplete interlayer bonding and residual voids near the lateral boundaries were observed, these defects were attributed to mold expansion and non-uniform compaction pressure rather than intrinsic process limitations. Feedstock-level compositional grading provides an alternative to process-level gradient control, enabling site-specific mechanical properties in AM components with reduced process complexity. Future work will focus on process optimization to improve consolidation quality and on integrating the feedstock into AM systems to demonstrate on-site property control in printed components.

Acknowledgments This research was developed with funding from the Defense Advanced Research Projects Agency (DARPA). The views, opinions and/or findings expressed are those of the authors and should not be interpreted as representing the official views or policies of DARPA or the U.S. Government.

References

1. Tammas-Williams, S., and I. Todd. “Design for additive manufacturing with site-specific properties in metals and alloys.” Scripta Materialia 135 (2017): 105-110.
2. Hofmann, Douglas C., Joanna Kolodziejska, Scott Roberts, Richard Otis, Robert Peter Dillon, Jong-Ook Suh, Zi-Kui Liu, and John-Paul Borgonia. “Compositionally graded metals: A new frontier of additive manufacturing.” Journal of Materials Research 29, no. 17 (2014): 1899-1910.
3. Yan, Lei, Yitao Chen, and Frank Liou. “Additive manufacturing of functionally graded metallic materials using laser metal deposition.” Additive Manufacturing 31 (2020): 100901.
4. Ding, Donghong, Zengxi Pan, Dominic Cuiuri, and Huijun Li. “Wire-feed additive manufacturing of metal components: technologies, developments and future interests.” The International Journal of Advanced Manufacturing Technology 81, no. 1 (2015): 465-481.
5. Yakubov, Vladislav, Halsey Ostergaard, Shishira Bhagavath, Chu Lun Alex Leung, James Hughes, Evren Yasa, Mani Khezri, Sandra K. Löschke, Qing Li, and Anna M. Paradowska. “Recycled aluminium feedstock in metal additive manufacturing: A state of the art review.” Heliyon 10, no. 5 (2024).
6. Riyad, M. Faisal, Pu Han, Shams Torabnia, and Keng Hsu. “Thermoacoustic Consolidation of Metal Particles for Energy-Efficient Metal Powders Recycling in Metal Additive Manufacturing.” Journal of Manufacturing Science and Engineering 147, no. 2 (2025): 021001.
7. Wheeler, J., Prior, D., Jiang, Z., Spiess, R., & Trimby, P. (2001). The petrological significance of misorientations between grains. Contributions to mineralogy and petrology, 141(1), 109-124.